A Unified Model of Optical and Physical Dot Gain in Printing

Li Yang
Campus Norrköping (ITN), Linköping University,
S-601 74, Norrköping, Sweden

Abstract

A unified model coping with both physical and optical dot gains on color tone reproduction of print is proposed. The physical dot gain, $\Delta\sigma$, is approximated by a quadratic function of nominal dot percentages, σ_0. The function, for each color, is characterized by a single parameter depending on printing technologies as well as ink-paper interactions, and has a symmetric form around $\sigma_0 = 50\%$. Applications to a color laser printer (on office copy paper) reproduces the experimental dot gain curves fairly well. Dependence on physical dot percentage, $\sigma = \sigma_0 + \Delta\sigma$, results in the optical dot gain and in turn the overall dot gain asymmetric forms, plotted against σ_0. Furthermore, theoretical analysis reveals fundamental differences between physical and optical dot gains.

Introduction

Color reproduction of printing is achieved by distributing (printing) colorants (inks, toners, etc.) onto a substrate surface. Ink setting on the surface is a complex process depending on the physical and chemical properties of the inks and the substrate, surface topology etc. In Electrophotographic systems, like laser printers, toner setting depends on toner transport and development (heating, fusing, and pressing) processes. In ink-jet systems, this depends on interaction between the ink drops and the surface of the printed media. Considering the relief structure of the printed page, the interaction results in ink spreading as well as ink penetration [1, 2].

Physical dot gain refers to a fact that sizes of printed dots differ from their nominal ones (bigger or smaller) in printing practices. Physical dot gain can be caused by printing systems, such as pressing force for toner setting, or by environment, for instance in ink jet printing, ink setting depends on moisture and surface state of substrates [3]. In a well controlled environment, physical dot gain may be considered as a systematic characteristic resulting from a printing system including printers and print-related materials. Therefore knowledge about physical dot gain of printing systems may be helpful in the system calibration and quality control of color reproduction.

Besides the physical dot gain that results from a real physical extension of an ink dot, there exists dot gain of optical origin [1, 4], i.e. optical dot gain or Yule-Nielsen effect. Optical dot gain results from light scattering inside the substrate, which leads to light exchanges between different chromatic areas, Σ_0 and Σ_1, as shown in Fig. 1. Because the light exchanges occur most possibly at regions close to the border between different chromatic areas, optical dot gain is closely related to the physical shape of the dots. Such a correlation between optical and physical dot gain makes the study a complicated task. Although there have been different approaches describing optical dot gain [5, 6, 7, 8, 9, 10, 11, 12, 13], experimental confirmation has been difficult because of difficulties in separating an optical dot gain from a physical one. Moreover quantitative evaluations to pure effects from physical dot gain or from optical dot gain has been difficult.

Co-existences of optical and physical dot gains in a print requires development for a unified model that accounts for both types of dot gain simultaneously. In previous publications [12, 13], we developed a model that parameterized optical dot gain in mono- and multi-color printing processes with considerations of ink penetration. In this work we present a model that parameterize physical dot gain. Based on these models a unified model characterizing both optical and physical dot gain is established. The model is further illustrated by applications to a laser printing system. Finally, correlations and fundamental differences between physical and optical dot gains are studied.

Methods

Parameterization of physical dot gain

Intuitively there exist correlations between the physical dot percentage, $\sigma = \sigma_0 + \Delta\sigma$, and the nominal one, σ_0. The correlation may mathematically be approximated by a polynomial expansion, for example a quadratic, i.e.,

$$\sigma = c + a\sigma_0 + b\sigma_0^2 \tag{1}$$

Considering constraints at $\sigma_0 = 0$ and 1, one gets,

$$\begin{aligned} c &= 0 \\ a + b &= 1. \end{aligned}$$

Then, Eq. (1) becomes,

$$\sigma = \sigma_0(a(1 - \sigma_0) + \sigma_0). \tag{2}$$

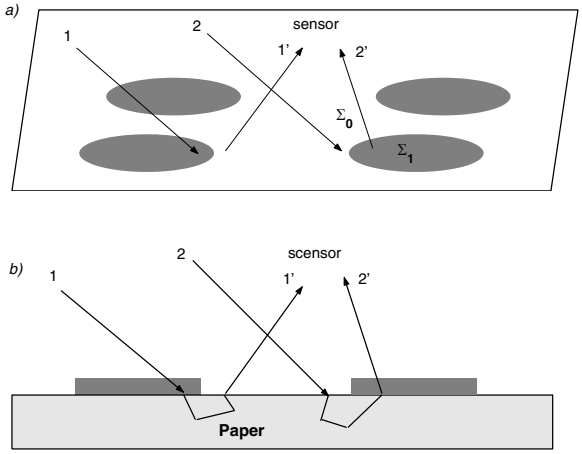

Figure 1: The Yule-Nielsen effect resulting from light scattering within the substrate. In the figure, light rays enter the substrate from one area (Σ_0 or Σ_1) and exit from another (Σ_1 or Σ_0).

Consequently, the expression of physical dot gain is,

$$\begin{aligned} \Delta\sigma &= \sigma - \sigma_0 \\ &= (a-1)\sigma_0(1-\sigma_0). \end{aligned} \quad (3)$$

This means that the physical dot percentage, σ, or in turn the physical dot gain, $\Delta\sigma$, can be parameterized by a single parameter, a, which depends on printing technologies (offset, or ink jet, etc.), printing materials (inks and substrates) used, and even printing environments, etc. Evidently, constraints for $\Delta\sigma = 0$ at $\sigma_0 = 0$ and 1, are automatically fulfilled in Eq. (3). The parameter, a, in Eq. (3) provides a measure to the physical dot gain. For example, $a = 1$ corresponds to no physical dot gain, while $a > 1$ or $a < 1$ stands for a physical dot extension ($\sigma > \sigma_0$) or a contraction ($\sigma < \sigma_0$), respectively.

Determination of physical dot gain from experimental data

Let the nominal dot percentage be σ_0 which becomes $\sigma = \sigma_0 + \Delta\sigma$ after printing, due to physical dot gain. According to our previous work [12, 13], the spectral reflectance values of a print can be computed from,

$$\begin{aligned} R(\sigma) &= R_{MD}(\sigma) - \Delta R_{opt}(\sigma) \\ &= R_{MD}(\sigma_0) - \Delta R_{phy}(\sigma_0) - \Delta R_{opt}(\sigma) \end{aligned} \quad (4)$$

where

$$R_{MD}(\sigma_0) = R_g(1-\sigma_0) + R_g T^2 \sigma_0 \quad (5)$$

is the term computed with Murray-Davis equation. R_g and T in Eq (5) refer to spectral reflectance and transmittance values of paper and ink layer, respectively. ΔR_{phy} and ΔR_{opt} in Eq. (4) correspond to contributions of physical and optical dot gain, respectively and are expressed as,

$$\begin{aligned} \Delta R_{phy}(\sigma_0) &= R_g T^2 \Delta\sigma \\ &= R_g T^2 (a-1)\sigma_0(1-\sigma_0) \quad (6) \\ \Delta R_{opt}(\sigma) &= \overline{p}(1-T)^2\sigma(1-\sigma) \quad (7) \end{aligned}$$

where $\overline{p}$ is an average probability for light exchange between Σ_0 and Σ_1 (see Fig. 1), due to light scattering in the substrate, and is defined as

$$\overline{p} = \frac{1}{\sigma(1-\sigma)} \int_{\Sigma_1} \int_{\Sigma_0} p(\mathbf{r_1}, \mathbf{r_0}) d\sigma_1 d\sigma_0. \quad (8)$$

In the equation, $p(\mathbf{r_1}, \mathbf{r_0})$ is the so-called point spread function (PSF) of the substrate, $\mathbf{r_0}$ and $\mathbf{r_1}$ denote positions where a photon enters and then exits the surface of the substrate. In case of complete light scattering, the photon has an identical probability to be scattered wherever in the substrate. Then, $\overline{p}$ is constant and independent of the incident and exiting positions [4, 12]. Consequently, the curve of optical dot gain, has a single maximum at $\sigma = 50\%$ and has a symmetric form around the maximum. Nevertheless, when there exists a physical dot gain, $\sigma \neq \sigma_0$, ΔR_{opt} becomes asymmetric around $\sigma_0 = 50\%$, plotted against the nominal dot percentage, σ_0, as one will see in Sec. .

Correlation of the optical dot gain, ΔR_{opt}, with the physical dot gain is clearly seen from Eq. (7), because of its dependence on $\sigma = \sigma_0 + \Delta\sigma$. Since physical and optical dot gain contribute simultaneously to reflective measurements, an overall effect of dot gain, ΔR, is actually measured, which is a superposition of their contributions, i.e.,

$$\Delta R = \Delta R_{phy} + \Delta R_{opt} \quad (9)$$

According to Eqs. (4-9), in addition to the optical properties of paper and ink, R_g, $\overline{p}$, T, etc., the spectral reflectance, R (or the overall dot gain, ΔR) is solely determined by the parameter, a. Therefore, by fitting to a set of experimental data, such as reflectance values or CIEXYZ tristimulus values, one can determine the quantity of a, and then the physical dot gain, $\Delta\sigma$.

ΔR_{phy} and ΔR_{opt} are mathematically similar, but their differences are significant. ΔR_{phy} is parabolic with respect to the nominal dot percentage, σ_0, but ΔR_{opt} to the total dot percentage, σ, instead. In other words, ΔR_{opt}, responses to the nominal (σ_0) as well as physical dot gain ($\Delta\sigma$), as a whole. Consequently, ΔR_{phy} and ΔR_{opt} are symmetric about their maxima at $\sigma_0 = 50\%$ and $\sigma = 50\%$, respectively, in the case of $\overline{p} = constant$ (i.e. light is completely scattered in the substrate). When ΔR_{opt} is plotted against the nominal dot percentage, σ_0, its maximum is shifted to a lower or higher σ_0 value, depending on $\Delta\sigma$ is positive or negative. Correspondingly, the total dot gain, ΔR, is asymmetric because it is a simple summation of the those two. Therefore, the asymmetry of the measured dot gain curve, ΔR, suggests the co-existence of physical and optical dot gain, as one can see in next Section.

Results and discussions

To illustrate applications of the model developed in the previous section, a laser printing system: HP Color Laser Jet 4500N was studied. Test patches of primary colors and black were printed by the printer with nominal dot percentages ranging from 0 to 100% and an interval of 5%. Ordinary office copy paper was used for printing. Settings for the printer were 600 dpi with scale patterns. Spectral reflectance values of the patches were obtained by utilizing a spectrophotometer (with an UV filter) which covers spectral wavelengths ranging from 380 to 730 nm and an interval of 10 nm. Spectral transmittance values of each color, T, is estimated by

$$T = (\frac{R_1}{R_g})^{1/2} \tag{10}$$

where R_1 is the spectral reflectance values of a full tone color. Applying Eq. (10), one must be aware of possible errors that may be associated with such a simple estimation. One of the possible errors comes from boundary reflections at air/ink and ink/paper interfaces which can be important for toner based colorants, because of different refraction indices of the ink and the air. One can cope with the boundary reflections by making the so-called Saunderson correction[14]. Another possible error relates with thickness variation of halftone dots. Determination of the thickness variation requires sophisticated microscopic studies[3], which is beyond the scope of this work. Fluorescence of the substrate can also be a source of error when an UV filter is not sufficient, as is the case of the present study. The simulation makes no attempt to exactly reproduce the measurement data rather to illustrate applications of the unified model. Nevertheless, since these possible errors are relatively less important compared to physical and optical dot gains, reasonable results of simulation can still expected.

Simulations were carried out by fitting the computed spectral reflectance values, R_{simu}, according to Eqs. (4-9), to the measurements, R_{exp}, in a sense of least squared error (LSQ), ie.,

$$Q = \sum_{\lambda} \sum_{\sigma} [R_{simu}(\sigma, \lambda) - R_{exp}(\sigma, \lambda)]^2. \tag{11}$$

Optical dot gain resulting from light scattering in substrate was approximated by the complete light scattering, and $\overline{p} = R_g$ was assumed in the simulation. Therefore, for each color, there is only one parameter, a, describing physical dot gain of printed dots, involved in fitting processes.

The dot gain curves

Figure 2 depicts variations of the physical dot gain, $\Delta\sigma$, and the physical (or real) dot percentage, σ, with respect to the nominal one, σ_0, for the primary colors as well as

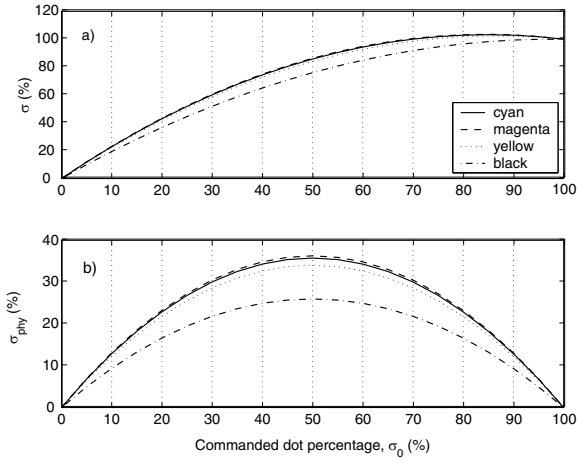

Figure 2: Variation of physical dot gain ($\Delta\sigma$) and printed dot percentage (σ) with respect to the nominal dot percentage (σ_0). Curves of cyan and magenta eventually overlap with each other.

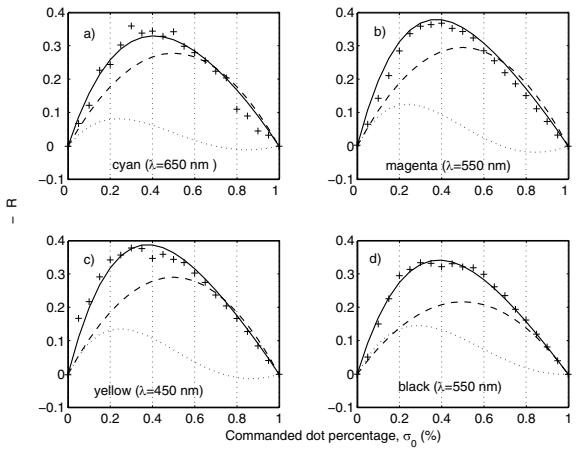

Figure 3: Effects of the physical (ΔR_{phy}), optical (ΔR_{opt}), and overall (ΔR) dot gain on reflectance values. Experimental values of ΔR are marked by +.

black. Figure 2a provides us with correlation between the actual dot percentages to theirs nominal values. As expected from the theoretical analysis, the physical dot gain (Fig. 2b) has a symmetric form about its maximum in mid tone, $\sigma_0 = 50\%$. The maximal physical gains range from $\Delta\sigma = 26\%$ to 36%, depending on colors. The dot gain is significant, particularly compared with its nominal value. Besides, cyan and magenta have eventually the same dot gain profile (they overlap with one another in the figure), while yellow and black have smaller and the smallest dot gain, respectively. The correspondent dot gain parameters are, a=2.4399 (cyan) 2.4338 (magenta), 2.2907 (yellow), and 2.0335 (black).

Figure 3 further demonstrates contributions from the physical and optical dot gain, ΔR_{phy} and ΔR_{opt}, and their joint effects on overall spectral reflectance values, ΔR. Because of spectral dependent, ΔR values corre-

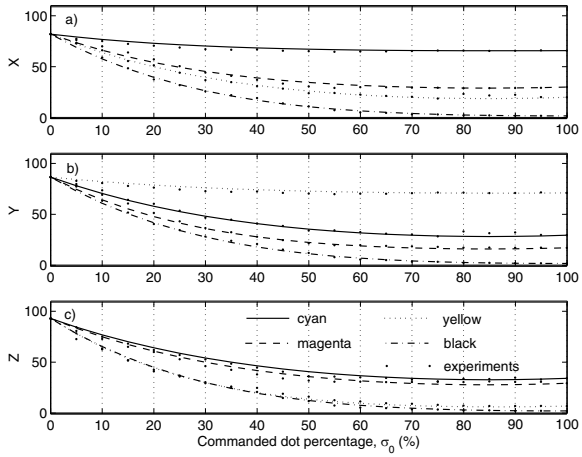

Figure 4: Simulated and measured (dots) CIEXYZ tristimulus values of cyan (solid lines), magenta (dashed lines), yellow (dotted lines), and black (dash-doted lines).

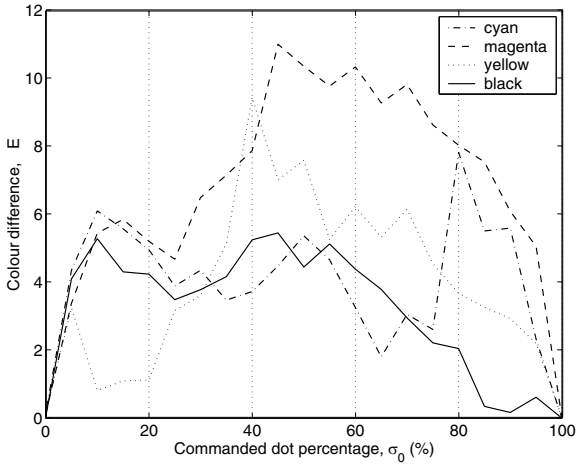

Figure 5: Color differences between simulated and measured spectra of cyan (solid lines), magenta (dashed lines), yellow (dotted lines), and black (dash-dot lines).

sponding to different nominal dot percentages and at a wavelength lying in the middle of the main absorption band of each color were plotted. At this wavelength (denoted in the figure), both the physical and optical dot gains have their maxima, which provide one with possible ranges for how much the effects of dot gains can be.

Due to physical extension of the printed dot, $\Delta\sigma > 0$, in the experiments, the optical dot gain reaches its maximum at about $\sigma_0 = 25\%$ to 30%, for the primary colors and black. Also due to physical dot gain, the print (tone) becomes eventually solid when the nominal dot percentage is $\sigma_0 \simeq 80\%$ or higher, which leads to the vanishing of the optical dot gain. Additionally, ΔR_{opt} shares a similar shape for all colors since their transmittance values at the wavelengths lying in the middle of their absorption bands are similar ($T \approx 0$). Finally, superpositions of the physical and optical dot gains make the overall dot gain, ΔR, an asymmetric shape with their maxima at about $\sigma_0 = 40\%$ for all colors. Experimental values of the overall dot gain are also included in Fig. 3, which agree fairly well with the simulations.

For a simpler comparison between the simulations and the measurements, both the simulated and experimental spectral reflectance values have been converted to their color coordinates in the $CIEXYZ$ color space. They are shown in Fig. 4, in which the simulations are represented by lines (solid, dashed, dotted, and dash-dot lines for cyan, magenta, yellow, and black, respectively) and the measurements by dots. The figure shows fairly good agreements between the simulations and the measurements, especially for X and Y. Figure 5 further provides a quantitative measure to the color differences between the simulated and experimental spectra. The plots show that for most of colors and dot percentages, the color differences lie below $\Delta E = 6$ except for magenta whose maximum is up to $\Delta E = 11$. This implies that the quadratic approximation to the physical dot gain (Eq. 14) and the assumption for complete light scattering hold reasonably well for this printing system. As suggested in the previous section, the error may come from the following possible sources: the boundary reflection, the thickness variation of ink dots, and even fluorescence of the substrate, which were ignored in this model. Studies to other printing systems are necessary in order that a general conclusion can be drawn.

Spectral dependence of the optical dot gain

Because $\Delta R_{opt} > 0$, the true reflectance of an image, R, is smaller than its Murray-Davies value, R_{MD}, and the halftone image appears to be darker (more saturated in color). Equivalently, it looks as though having a larger dot percentage than it physically is. For this reason this effect is known as optical dot gain.

In cases of complete light scattering, $\overline{p} = C$ (a constant and $C \leq 1$), which corresponds to the Yule-Nielsen model with a Yule-Nielsen factor, $n = 2$ [12]. Correspondingly, the dot gain has its maximum at $\sigma = 50\%$, i.e.,

$$(\Delta R_{opt})_{max} = (1 - T)^2 C/4 \qquad (12)$$

In an extreme case, $T = 0$ and $C = 1$, one gets the biggest possible optical gain, $\Delta(R_{opt})_{max} = 0.25$.

The term of optical dot gain may give one such an impression that it may be possible to represent an optical dot gain by a physical dot extension. If so, it would be possible to compensate the optical dot gain by making precorrections to an original. Consequently, a perfect tone reproduction would be achievable. Unfortunately, the following analysis will show that such a compensation is not fully applicable over a whole spectrum, because of fundamental differences between optical dot gain and physical one.

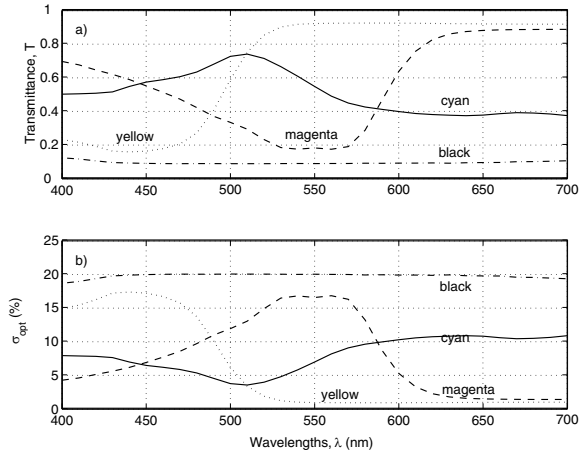

Figure 6: Spectral dependence of the pretended physical dot extension, $\Delta\sigma_{opt}$, resulting from effects of light scattering in the substrate. In the calculation, $\sigma = 0.4$ and the complete light scattering was assumed. a) spectral transmittance values of the toners; b) computed values of $\Delta\sigma_{opt}$ according to Eq. (12).

As an attempt to correlate effects of optical dot gain with a physical dot extension, $\Delta\sigma_{opt}$, one may consider the measured reflectance of dot percentage σ, $R(\sigma)$, as if it is originated from a dot size of $\sigma + \Delta\sigma_{opt}$. Therefore, let

$$\begin{aligned} R(\sigma) &= R_{MD}(\sigma) - \Delta R_{opt}(\sigma) \\ &= R_{MD}(\sigma + \Delta\sigma_{opt}) \\ &= R_{MD}(\sigma) - R_g(1 - T^2)\Delta\sigma_{opt}. \end{aligned} \quad (13)$$

Applying expressions for R_{MD} and ΔR_{opt} (Eqs. (5) and (7)) one obtains,

$$\begin{aligned} \Delta\sigma_{opt} &= \frac{\Delta R_{opt}}{R_g(1 - T^2)} \\ &= \frac{(1 - T)\overline{p}}{(1 + T)R_g}\sigma(1 - \sigma) \end{aligned} \quad (14)$$

Clearly, $\Delta\sigma_{opt}$ is a function of the optical properties (T, R_g) of the materials as well as ink percentage (σ). Due to spectral dependence, $\Delta\sigma_{opt}$ has its maxima in absorption bands where T is small but minima in transparent bands (where $T \to 1$). This makes an optical dot gain differ fundamentally from a physical dot gain. Therefore, unless for an ideal black, $T = 0$, an optical dot gain can not be properly represented by any single physical dot extension over the whole spectrum, even for primary colors. To further demonstrate the spectral dependence, optical dot gains computed with to Eq. (12) is depicted in Fig. 6. In the calculation, $\sigma = 0.4$ and a complete light scattering was assumed. Clearly, $\Delta\sigma_{opt}$ shows a distinct correlation with its spectral transmittance, and the quantity $\Delta\sigma_{opt}$ varies significantly with the wavelengths.

Remarks

Along with three other spectral models: Clapper-Yule multiple internal reflections model, Beer-Bouger law, and Kubelka-Munk theory, Yule-Nielsen model expressed as[15, 16]

$$R(\lambda)^{\frac{1}{n}} = \sum_{i=1}^{N} w_i R(\lambda)^{\frac{1}{n}} \quad (15)$$

is possibly the most commonly used model[17]. The factor, n, is called the Yule-Nielsen factor and is derived from best fit for the model to measurement data. The Yule-Nielsen (Y-N) equation is an empirical power-law correction to Murray-Davies model corresponding to $n = 1$. According to Ruchdeschel and Hauser[18], $1 \leq n \leq 2$, when only optical dot gain accounts. This modification originally aimed at accounting for effects of optical dot gain. Unfortunately, difficulties in separating physical dot gain from the optical one make the preassumption of the Y-N equation seldom fulfilled in applications. Consequently, the empirically derived Y-N factor can be significantly bigger than 2. For example, for a print created by an ink-jet, possessing significant physical dot gain due to ink spreading, the best fit Yule-Nielsen factor[19] can be up to $n = 10$.

Numerous researchers have made great efforts to improve numerical accuracy of the Yule-Nielsen corrected Murray-Davies models, applied to predict spectral distributions and tristimulus values of color halftones [20, 21, 22, 23, 24, 25, 26]. However, these improvements build on introducing more $Y - N$ factors in regression processes, as for instance cellular Y-N models[24, 25, 26, 27], and therefore, does not provide more physical insights into problems. Because of the co-existence of both physical and optical dot gains in measurement data, the empirically derived Y-N factors, n, has no direct (or not much) physical meaning on their own. Moreover, as increasing popularity of paper containing fluorescent whitening agents (FWAs), physical interpretations of Y-N factors become even less clearer.

Comparatively, the present model builds on a solid physical ground, in which every parameter has a direct physical meaning on its own. It provides one with insides into problems studied. For example, determination of physical dot gain can be used to calibrate printers that may even be helpful for printer developments and halftoning. Moreover, such a model building strategy makes ease of model extensions to include other physical effects like fluorescence of a substrate, boundary reflection, etc. Detailed descriptions of an extension to prints on a substrate containing FWAs will be reported elsewhere[28]. On the other hand, this allows one to test the model experimentally, by isolating one effect from others.

Summary

A model coping with both physical and optical dot gains in tone reproduction is derived. In the model, physical dot gain is approximated by a quadratic function of nominal dot percentage. For each color, the function is characterized by a single parameter depending on printing technologies as well as ink-paper interactions. The parameter can be derived by fitting to experimental data, say, spectral reflectance values of a set of test patches. The model reveals that physical dot gain, $\Delta\sigma$, has a parabolic form, plotted against nominal dot percentage (σ_0), and reaches its maximum around $\sigma_0 = 50\%$. The response (dependence) of the optical dot gain to the physical dot gain (dot extension) results in an asymmetric form of the optical dot gain, in turn, an asymmetric form of the overall dot gain. The model is applied to a color laser printer. The simulated dot gain curves are in fairly good agreement with measurements. Theoretical analysis suggests that it is impossible to represent an optical dot gain by any single physical dot extension over the whole visible spectrum, because of spectral dependence of the optical dot gain.

Acknowledgement

This work is supported by Swedish Foundation for Strategic Research through Surface Science Printing Program (S2P2).

References

1. L. Yang. *Ink-Paper Interaction: A study in ink-jet color reproduction*. Ph.D thesis, Dissertation No. 806, Linköping University, Sweden (2003).
2. S.S Hwang. Toner penetration into paper at fusing. *J. Imaging Sci. Technol.*, **44**: 26 (2000).
3. P. Emmel and R.D. Hersch. Modeling ink spreading for color prediction. *J. Imaging Sci. Technol.*, **46**: 237 (2002).
4. G.L. Rogers. Optical dot gain in a halftone print. *J. Imaging Sci. Technol.*, **41**: 643 (1997).
5. J.S. Arney. A probability description of the Yule-Nielsen effect, i. *J. Imaging Sci. Technol.*, **41**: 633 (1997).
6. J.S. Arney and M. Katsube. A probability description of the Yule-Nielsen effect ii: The impact of halftone geometry. *J. Imaging Sci. Technol.*, **41**: 637 (1997).
7. A.C. Hübler. The optical behavior od screened images on paper with horizontal light diffusion. In *IS&T's NIP-13: International Conference on Digital Printing Technologies*. TREK INCORPORATED, New York (1997).
8. S. Gustavson. *Dot Gain in Color Halftones*. Phd thesis, Dissertation No. 492, Linköping University, Sweden (1997).
9. G.L. Rogers. Effect of light scatter on halftone color. *J. Opt. Soc. Am. A*, **15**: 1813 (1998).
10. G.L. Rogers. Optical dot gain: lateral scattering probabilities. *J. Imaging Sci. Technol.*, **42**: 341 (1998).
11. P. Emmel and R.D. Hersch. A unified model for color prediction of halftoned prints. *J. Imaging Sci. Technol.*, **44**: 351 (2000).
12. L. Yang, R. Lenz, and B. Kruse. Light scattering and ink penetration effects on tone reproduction. *J. Opt. Soc. Am. A*, **18**: 360 (2001).
13. Li Yang, Sasan Gooran, and Björn Kruse. Simulation of optical dot gain in multichromatic tone production. *J. Imaging Sci. Technol.*, **45**: 198 (2001).
14. J.L. Saunderson. Calculation of the color pigmented plastics. *J. Opt. Soc. Am.*, **32**: 727 (1942).
15. J.A.C. Yule and W.J. Nielsen. The penetration of light into paper and its effect on halftone reproduction. *TAGA Proceeding*, **3**:65 (1951).
16. J. A. Viggiano. The color of halftone tints. In *TAGA Proc.*, pp. 647–661 (1985).
17. A.U. Agar. Model Based Color Color Separation for CMYKcm Printing. In *Proc. International Conf. Image Processing (ICIP 2000) and references therein*. IEEE Computer Society,. Vancouver, BC, Canada (2000).
18. F.R. Ruckdeschel and O.G. Hauser. Yule-Nielsen effect in printing: a physical analysis. *Appl. Opt.*, **17**: 3376 (1978).
19. R. S. Berns, A. Rose, and D. Y. Tzeng. The spectral modeling of large-format ink-jet printers. Research and development final report, RIT Munsell Color Science Laboratory (1996).
20. K. J. Heuberger, Z. M. Jing, and S. Persiev. Color transformations and lookup tables. In *TAGA&ISCC Proc.*, pp. 863–881 (1992).
21. R. Rolleston and R. Balasubramanian. Accuracy of various types of neugebauer model. In *Proc. of the First IS&TSID Color Imaging Conf.*, Scottsdale, AZ, pp. 32–37 (1993).
22. B. K. Lee. Estimation of the neugebauer model of a halftone printer and its applications. In *IS&TOSA Optics & Imaging in the Information Age Proceedings*, pp. 376–379 (1996).
23. R. R. Balasubramanian. The use of spectral regression in modeling halftone color printers. In *IS&TOSA Optics & Imaging in the Information Age Proceedings*, pp. 372–375 (1996).
24. S. L. Chang, Y. T. Liu, and D. Z. Yeh. A model to estimate fractional areas of neugebauer primary colors. In *Proc. of the Fifth IS&TSID Color Imaging Conf.*, Scottsdale, AZ, pp. 97–100 (1997).
25. C. C. Hua and K. L. Huang. Advanced cellular YNSN printer model. In *Proc. of the Fifth IS&TSID Color Imaging Conf.*, Scottsdale, AZ, pp. 231–234 (1997).
26. A. U. Agar and J. P. Allebach. A iterative cellular YNSN method for color printer characterization. In *Proc. of the Fifth IS&TSID Color Imaging Conf.*, Scottsdale, AZ, pp. 197–200 (1997).
27. T. Ogasahara. Optimization of the predicting model for dye-based inkjet printer. In *IS&T's NIP-19: International Conference on Digital Printing Technologies*, eds. IS&T, Springfield,VA, pp. 785–788 (2003).
28. L. Yang. Spectral model of halftone on a fluorescent substrate. to be submitted.

Biography

Li Yang received his Ph.D in Media Technology, in Linköping University, Campus Norröping, in April 2003. He continue working as a researcher in the Group of Media Technology. His research aims at model-building and simulation in Paper Optics and Graphic Arts, including ink-paper interaction, fluorescence, physical and optical dot gain, etc. He is a member of Is&T and TAGA. More information may be found on my web page at http://www.itn.liu.se/∼liyan/ or by sending email: liyan@itn.liu.se